

PACS numbers: 52.77.Dq; 52.50.Jm; 42.65.Re
DOI: 10.1070/QE2005v035n01ABEH002754

Implantation of high-energy ions produced by femtosecond laser pulses

R.V. Volkov, D.M. Golishnikov, V.M. Gordienko, A.B. Savel'ev, V.S. Chernysh

***Abstract*. Germanium ions of an expanding plasma were implanted in a silicon collector. The plasma was produced by a femtosecond laser pulse with an intensity of $\sim 10^{15}$ W cm^{-2} at the surface of the solid-state target. A technique was proposed for determining the energy characteristics of the ion component of the laser plasma from the density profile of the ions implanted in the substrate.**

Keywords: *femtosecond pulses, laser plasma, implantation, high-energy ions.*

1. Introduction

The plasma produced by an ultrashort laser pulse of a superstrong light field at the surface of a solid-state target is a unique source of high-energy ion and electron beams [1]. When femtosecond laser radiation with a high contrast ratio and an intensity of $10^{15} - 10^{16}$ W cm^{-2} interacts with a solid target, a high-energy ion component (above 10 keV) is formed in the laser plasma. The kinetic energy of ions, the degree of their ionisation, the directivity pattern, and the elemental composition of the expanding plasma depend not only on the parameters of the laser radiation (intensity, pulse duration, wavelength, energy contrast ratio), but on the state of the target surface as well. In this case, by modifying the target surface layer, it is possible to control the plasma parameters [2, 3].

The fast ion beams formed in the course of superintense laser radiation – matter interaction may be employed in the development of new ion implantation technologies. The conventional technology of ion implantation by an accelerated ion beam enables introducing a controllable amount of impurity atoms into the target surface layer and therefore leads to a modification of the physical and chemical properties of the surface layer in different materials.

A combined technique of ion implantation was described in Ref. [4], where the material ionisation was produced by a nanosecond laser pulse and the subsequent ion acceleration to high energies was producted by an electrostatic field. Direct implantation of ions from a laser-produced plasma without using the accelerating potential was realised employing the third harmonic of iodine laser radiation ($\lambda = 1.315$ μm) at a pulse duration of 400 ps and an intensity up to 10^{16} W cm^{-2} [5]. Going over to femtosecond superstrong-field repetitively pulsed laser systems will permit producing directional higher-energy ion beams and implanting ions deeper in the material. In experiments of this kind, laser-induced implantation shows promise for the modification of the target surface layer and at the same time can be a method for the investigation of ion energy spectrum and angular ion distribution. As a diagnostic tool, ion implantation can also be employed in experiments in the generation of thermonuclear neutrons from solid-state targets with simultaneous determination of ion energy distribution averaged over a large number of shots.

The aim of our work is to demonstrate the potentialities of laser-induced implantation employing high-intensity femtosecond pulses and to determine the potential applicability of this technique for characterising the energy spectrum of laser-produced plasmas.

2. Experiment on direct laser-induced germanium ion implantation in silicon

The experimental setup for laser-induced germanium ion implantation in a silicon substrate is shown in Fig. 1. We employed single crystal Ge as a target, and a Si plate with the $\langle 100 \rangle$ orientation served as an ion collector. The target was placed in a vacuum chamber evacuated to a residual gas pressure of 10^{-5} Torr.

The target was irradiated by dye laser pulses with $\lambda = 616$ nm, a duration $\tau = 200$ fs, and an energy of 200 – 300 μJ. The radiation was focused with a lens with a focal length of 11 cm to provide a radiation intensity of $(0.5 - 3.5) \times 10^{15}$ W cm^{-2} at the target. The measured diameter of the laser beam waist was equal to 7 ± 1 μm. In our experiments, the distance between the silicon collector and the germanium target was equal to 1.5 ± 0.2 cm. The germanium target was irradiated by 1.5×10^3 laser pulses. The focusing of laser radiation on the target was monitored from the X-ray radiation yield employing NaI(Tl) X-ray detectors. The laser pulse interacted primarily with a laser-modified target (with laser-produced craters) [2]. The first laser pulse formed a crater on the target surface and the subsequent pulses interacted with a strongly developed crater surface. The same point on the

R.V. Volkov, D.M. Golishnikov, V.M. Gordienko, A.B. Savel'ev International Teaching and Research Laser Center, M.V. Lomonosov Moscow State University, Vorob'evy Gory, 119992 Moscow, Russia; e-mail: golishnikov@femtosrv.phys.msu.su;
V.S. Chernysh Department of Physics , M.V. Lomonosov Moscow State University, Vorob'evy gory, 119992 Moscow, Russia

Received 6 July 2004
Kvantovaya Elektronika **35** (1) 33 – 37 (2005)
Translated by E.N. Ragozin

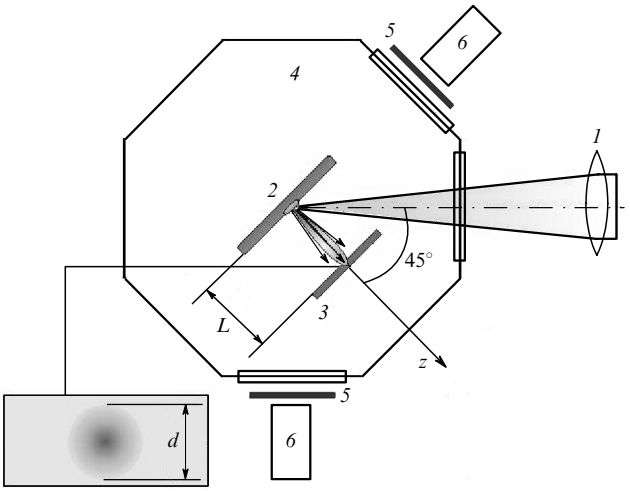

Figure 1. Scheme of the experiment on laser-induced ion implantation: (*1*) focusing lens; (*2*) target; (*3*) collector; (*4*) vacuum chamber; (*5*) Al and Be filters; (*6*) NaI(Tl) X-ray detectors; $L = 1.5 \pm 0.2$ cm is the distance between the target and the collector; the inset at the left schematically shows the implanted collector region ($d \sim 5$ mm is the diameter of the implanted region).

target was irradiated by 10 – 15 laser pulses. After this series of pulses, the yield of X-ray radiation from the plasma began to decrease because of displacement of the laser beam waist from the exact focus position, and then the target was displaced. 100-μm thick Be and Al filters were placed in front of the detectors. Their 1-% transmittance corresponds to a photon energy of 5 keV for the Al filter and to 1.34 keV for the Be filter [6]. No photons with energies higher than 5 keV were detected upon irradiation of a flat germanium surface. However, for the same intensity ($\sim 10^{15}$ W cm^{-2}), we recorded X-ray with a photon energy above 5 keV from the plasma of the modified germanium target. This allowed us to measure the characteristic energy of the hot electron component in the plasmas of modified targets (using technique [7] which we proposed earlier), which was found to be 1.5 ± 0.6 keV.

After implantation by germanium ions, the silicon collector was investigated by the methods of secondary ion mass spectrometry (SIMS) and Rutherford backscattering (RBS). The SIMS analysis was performed with a Cs ion beam with an energy of 7 keV for an ion current density of 9.05×10^{13} particle cm^{-2} and a residual gas pressure in the vacuum chamber of $\sim 10^{-9}$ Torr. When analysing the implanted collector by the RBS technique, we used a 2-MeV He^+ ion beam. The cross section of the probe beam was 1 mm × 2 mm. The collector surface was also studied with a scanning electron microscope.

3. Experimental results

The analysis of the of SIMS data gave the density profile of Ge atoms in the silicon matrix. Figure 2 shows this profile after 1500 laser shots for a region of collector surface of size 400 μm × 400 μm. The ion signal was calibrated in depth by measuring the depth of the crater produced by the ion beam, and the calibration in density was accomplished by comparing the ion signal from the implanted SiGe sample with the known density profile of Ge atoms in a silicon matrix.

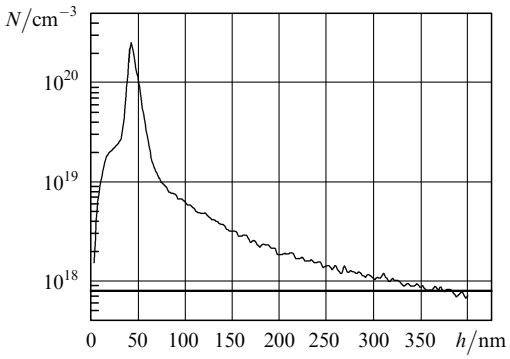

Figure 2. Density profile $N(h)$ of germanium atoms in the silicon matrix determined at the centre of the spot of implanted atoms. The horizontal line shows the threshold of ion detection by the SIMS technique.

The horizontal line in Fig. 2 indicates the ion detection threshold. The densities below a certain threshold ($\sim 10^{-5}$ of the solid-state density) turn out to be unreliable, and so weak an ion signal may arise from ion clusters with a mass equal to the Ge ion mass. Therefore, the maximum penetration depth of implanted atoms does not exceed 400 nm, which limits the maximum range of the diagnostic technique. Figure 3 shows the densities of Ge and Si atoms as functions of sputtering time t (the number of sputtered ions recorded in a second) determined by the SIMS technique, which allow one to compare the behaviour of these densities near the implanted collector boundary.

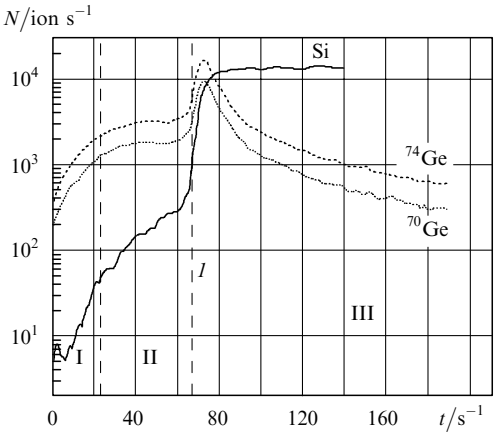

Figure 3. Density profile of Ge and Si atoms in the silicon matrix. Region I is the transition layer of surface contamination, region II is the Ge surface film, region III is the implanted domain, line (*1*) is the boundary of the silicon plate prior to implantation.

The backscattered-ion spectrum is shown in Fig. 4a. The peak about the 390th channel corresponds to the existence of a surface germanium film and the elongated 'tail' corresponds to germanium atoms introduced into the silicon matrix. The results of spectrum processing obtained with the help of the RUMP code [8] are given in Fig. 4b. One can see that the signal corresponding to the scattering by germanium ions was detected even up to a distance of 0.6 μm from the collector surface. Note that the same RBS spectrum in the channels having numbers 260 – 380 may be due to the existence of germanium clusters with a characteristic size of

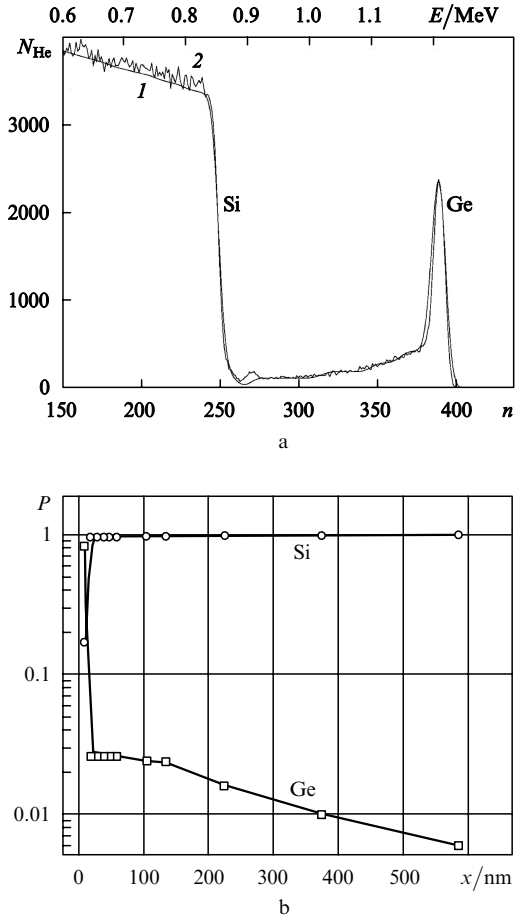

Figure 4. Energy spectrum of backscattered helium ions [curve (*1*) corresponds to the model described by Fig. 4b and curve (*2*) represents experimental data] (a) and density profiles of Ge and Si atoms in the silicon matrix which adequately describe the experimentally observed spectra and correspond to curve (*1*) in Fig. 4a (b) (E is the energy of scattered particles, N_{He} is the number of counts during the observation time, n is the channel number, x is the distance from the target surface, and P is the element fraction).

~ 1 μm on the collector surface. It is well known that macroscopic material droplets may emanate from the collector surface in the laser ablation of solid-state targets.

The implanted collector surface was investigated with the help of an electron microscope. One can see from Fig. 5 that macroscopic clusters with transverse dimensions of ~ 2 μm are observed on the collector surface. The average distance between them was equal to 100 – 500 μm. At the same time, such clusters were not found when recording the surface profilogram of the crater (400 μm× 400 μm) produced by the Cs ion beam during SIMS measurements of the density profile.

4. Discussion of experimental results

As shown by ion spectra measurements [9] performed with a time-of-flight mass spectrometer for a laser radiation intensity of $\sim 10^{16}$ W cm^{-2}, the ions in the laser plasma may have the degree of ionisation up to $Z = 6$, and their kinetic energy at a distance of 62 cm from the target may amount to 150 keV. In this case, the angular ion distribution with the use of planar targets is rather narrow and

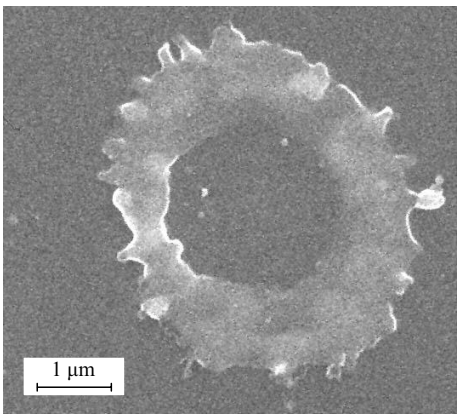

Figure 5. Photograph of a separate germanium surface cluster on a silicon collector obtained with a scanning microscope.

directed along the normal to the target plane. The ion energy distribution is adequately described by the exponential law $N(E) \sim \exp(-E/T_h^i)$, where T_h^i is the temperature of the hot ion component, which is determined by the temperature of the hot electron component of the laser plasma and the charge-state composition of the plasma: $T_h^i \approx ZT_h^e$ [1]. The temperature T_h^e of the germanium target measured in our experiment was 1.5 ± 0.6 keV. Therefore, for the average degree of ionisation in the plasma $Z = 6$ achievable at an intensity of $(1-3) \times 10^{15}$ W cm^{-2}, the temperature of the hot ion component of the plasma can be estimated as $T_h^i \sim 10$ keV.

By using the SRIM code [10], it is possible to estimate the average projective range (penetration depth) and calculate the implanted ion density profile for an ion beam with an energy of 10 keV.

During the ion implantation, the low-energy ions and neutral atoms of the expanding plasma form a thin film on the collector surface. At a point in Fig. 3 corresponding to the sputtering time $t = 60$ s, one can see a boundary between the germanium film and the silicon substrate. Several layers can be distinguished in the target (see Fig. 3). The first layer, which is characterised by a lowering of germanium density, is the upper transition layer of surface contamination (the film of oxides, organic contamination, and water). It is followed by a layer with constant germanium density – a germanium film on the silicon surface produced by low-energy ions. The third layer begins after a stepwise rise in silicon density – the initial collector boundary prior to implantation. This is an implanted layer, it is characterised by a sharp decrease in the density of implanted atoms; the atomic density profile has a peak, which corresponds to the germanium film – silicon interface. The interface in Fig. 3 corresponds to a depth of 30 – 40 nm (Fig. 2). When determining the ion energy characteristics from the implanted-ion distribution profile, the first 30 – 40 nm of the surface film should not be taken into account. The density peak of Ge atoms is located at a depth of ~ 120 Å from the interface between the silicon substrate and the germanium film. The reasons underlying the choice of this thickness of the surface film are explained below.

The initial integral equation, which is to be numerically solved to reconstruct the ion spectrum from the density profile (the homogeneous Fredholm equation of the first

kind [11]), does not have a unique solution. In this case, the problem itself is ill-posed, but it can be solved numerically under certain restrictions [12]. Nevertheless, the experimental density profile of implanted ions permits determining some energy characteristics of the plasma ion spectrum without using powerful numerical calculations.

Because Ge and Si are materials which can interdiffuse under specific conditions, in the processing of experimental data on laser-induced Ge implantation in Si one should consider the possible effect of diffusion on the Ge ion distribution in the silicon substrate. An analysis of the data published in the literature [13–16] shows that the diffusion of silicon into germanium (and in the opposite direction) turns out to be significant at temperatures close to 1000 °C and proceeds rather slowly even at these temperatures [13]. Therefore, when processing the SIMS data, we will neglect the interdiffusion of Ge and Si atoms, because the diffusion at room temperatures proceeds slowly and inefficiently.

We determined the distribution of implanted ions over the depth by using the SRIM code, which relies on the quantum-mechanical description of the collision of a monochromatic beam of implanted ions with the atoms of a substrate. With this code, we calculated the average projective range of germanium ions in silicon as a function of beam energy.

To compare the experimental density profile of germanium atoms in the silicon substrate (Fig. 2) and the calculated densities for a monochromatic ion beam (Fig. 6), it is necessary to calculate the thickness of the surface film. In our experiments, the resolution of the RBS technique in depth was equal to 120 Å. Processing the recoil nuclei signal suggests that the thickness of the surface germanium film does not exceed the resolution of this technique, i.e. 120 Å. At the same time, the SIMS data yield a film thickness of 305 Å. Note that a surface film and a bulk sample differ dramatically (in some instances by an order of magnitude [17]) in sputtering rate. The signal in Fig. 2 was calibrated in depth by dividing the crater depth by the sputtering time, and the effect of the surface film was therefore disregarded. Therefore, the surface film thickness was incorrectly calculated by the SIMS technique [18].

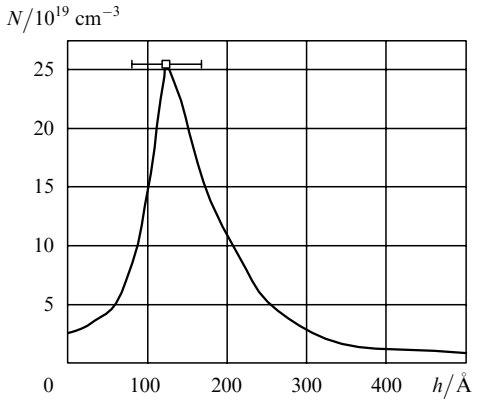

Figure 6. Experimental Ge ion density in the silicon collector N versus depth h (solid curve) and calculated projective range of a monochromatic germanium ion beam with an energy of 10 keV (□). The surface film thickness is taken to be equal to 305 Å, which coincides with the RBS data by the order of magnitude.

A characteristic property of direct laser-induced implantation is a broad expanding-plasma ion spectrum, which depends only slightly on experimental conditions. That is why direct laser-induced implantation in our experiments can also be considered as a method of diagnostics of the ion plasma component. As shown in Ref. [5], this technique is in qualitative agreement with the time-of-flight ion mass spectrometry technique. The advantages of this method are evident: it is simple and yields information on the ion energy spectrum averaged over ten thousands of laser shots. The latter circumstance is especially significant in laser-plasma experiments performed with a high pulse-repetition rate. For instance, in the experiments on the detection of thermonuclear neutrons escaping from the laser plasma of deuterated targets described in Ref. [19], 2000–5000 laser shots were required for a trustworthy determination of the neutron yield, the neutron yield depending on the energy and spectrum of deuterium ions. An ion collector accommodated in the experimental chamber will provide a passive monitoring of the energy spectrum of the ejected ions. The averaged ion energy data obtained in this way could be compared with the estimates made on the basis of the measured neutron yield.

Therefore, our work demonstrates the feasibility of germanium ion implantation in a silicon substrate using femtosecond laser pulses with an intensity of 10^{15}–10^{16} W cm^{-2}. Implanted germanium ions were found in the substrate material at depths up to 400 nm. The average energy of the ion component of the expanding laser-produced plasma can be determined from the density profile of implanted ions.

Acknowledgements. The authors thank M.A. Timofeev and V.S. Kulikauskas for their assistance in carrying out the work on electron microscopy and RBS. This work was supported by the Russian Foundation for Basic Research (Grant No. 02-02-16659).

References

1. Luther-Davis W., Gamalii E.G., Wang Yanji, Rode A.V., Tikhonchuk V.T. *Kvantovaya Elektron.*, **19** (4), 317 (1992) [*Quantum Electron.*, **22** (4), 289 (1992)].
2. Golishnikov D.M., Gordienko V.M., Mikheev P.M., et al. *Laser Phys.*, **11**, 1205 (2001).
3. Volkov R.V., Gavrilov S.A., Golishnikov D.M., Gordienko V.M., Mikheev P.M., Savel'ev A.B., Serov A.A. *Kvantovaya Elektron.*, **31** (3), 241 (2001) [*Quantum Electron.*, **31** (3), 241 (2001)].
4. Bykovskii Yu.A., Nevolin V.N., et al. *Ionnaya i lazernaya implantatsiya metallicheskikh materialov* (Ion and Laser Implantation of Metallic Materials) (Moscow: Energoatomizdat, 1991).
5. Torrisi L., Gammino S., Mezzasalma A.M., et al. *Appl. Surf. Sci.*, **217**, 319 (2003).
6. http://www-cxro.lbl.gov/optical_constants/filter2.html.
7. Volkov R.V., Gordienko V.M., Mikheev P.M., Savel'ev A.B. *Kvantovaya Elektron.*, **30** (10), 896 (2000) [*Quantum Electron.*, **30** (10), 896 (2000)].
8. http://www.mse.cornell.edu/cgs, http://www.genplot.com/RUMP/index.htm.
9. Volkov R.V., Golishnikov D.M., Gordienko V.M., et al. *Kvantovaya Elektron.*, **33** (11), 981 (2003) [*Quantum Electron.*, **33** (11), 981 (2003)].
10. Ziegler J.F., Biersack J.P., Littmark U. *The Stopping and Ranges of Ions in Solids* (New York: Pergamon Press, 1985).
11. Vasil'eva A.B., Tikhonov A.N. *Integral'nye uravneniya* (Integral Equations) (Moscow: Izd. MGU, 1989).

12. Tikhonov A.N., Arsenin V.Ya. *Solutions of Ill-Posed Problems* (New York: Halsted Press, 1977; Moscow: Nauka, 1974).
13. Ronning C., Carlson E.P., Davis R.F. *Phys. Rep.*, **351**, 349 (2001).
14. Strohm A., Voss T., Frank W., et al. *Physica B*, **308–310**, 542 (2001).
15. Kim K., Kim H.S., Kim J.Y., et. al. *J. Solid State Electrochem.*, **1**, 221 (1997).
16. Jiang Z., Xu A., Hu D., et al. *Thin Solid Films*, **321**, 116 (1998).
17. Behrisch R. (Ed.) *Sputtering by Particle Bombardment* (Berlin, New York: Springer-Verlag, 1981; Moscow: Mir) Vol. I, Ch. 4.
18. Behrisch R. (Ed.) *Sputtering by Particle Bombardment* (Berlin, New York: Springer-Verlag, 1991; Moscow: Mir) Vol. III.
19. Volkov R.V., Golishnikov D.M., Gordienko V.M., et al. *Pis'ma Zh. Eksp. Teor. Fiz.*, **72**, 577 (2000).